Proceedings of the 9th World Congress on Mechanical, Chemical, and Material Engineering (MCM'23)
Brunel University, London, United Kingdom –August 06-08, 2023
Paper No. 219
DOI: 10.11159/htff23.219

Effect of Static Liquid Height on Gas Holdup of a Bubble Column Reactor

M. W. Abdulrahman[1], N. Nassar[2]
[1]Rochester Institute of Technology (RIT)
Dubai, UAE
mwacad@rit.edu; nin8507@g.rit.edu
[2]Rochester Institute of Technology (RIT)
Dubai, UAE

Abstract –In this paper, the hydrodynamics of a direct contact heat transfer in a Bubble Column Reactor are investigated using a three dimensional, Eulerian-Eulerian Computational Fluid Dynamics (CFD) model. In particular, the effect of the static liquid (H) height on gas holdup (α_g) is examined by using three different heights (45, 55, and 65 cm). Using experimental data, the model is validated and compared to a previous two-dimensional CFD model. It is found that the three-dimensional system can precisely model the trends of gas holdup as the static liquid height height changes. In addition, compared to the 2D model, the 3D model is more precise and overestimated the gas holdup. In addition, increasing the static liquid height causes the gas holdup to decrease; where the gas holdup decreases by 11% when the static liquid height increases from 45cm to 65cm.

Keywords**:** gas holdup; hydrodynamics; static liquid height; CFD; 3D

1. Introduction

It is anticipated that hydrogen will be a major contributingcomponent to the sustainable energy supply in the future [1] since the usage of hydrogen will minimize the pollution that contributes to climate change by lowering greenhousegas emissions. Hydrogen gas generation from a variety of fuel gases may create greenhouse gases, however the emissions are much lower than those typical produced by gasoline and diesel vehicles. Thermochemical cycles are prospective solutions that can be coupled with nuclear reactors in order to thermally decompose water into oxygen and hydrogen via multistage processes. The copper-chlorine (Cu-Cl) cycle has been identified by Argonne National Laboratories (ANL) as one of the most promising low temperature cycles [2], [3].

The oxygen reaction in the Cu-Cl cycle of hydrogen production is a high temperature reaction that requires a source of high temperature heat. This heat may be generated using nuclear reactors or solar thermal energy which are non-polluting source of high-temperature heat. It has been found that the more practical and effective method of heating oxygen reactor is to heat the molten salt inside the oxygen reactor, which will transmit heat from the molten CuCl to the solid Cu2OCl2 (reactant) particles within the reactor. Different mechanisms of heat transfer for the oxygen reactor have been investigated [4-8]. It has been determined that direct contact heat transfer from the oxygen gas to the molten CuCl is the optimal heat transfer mechanism for the oxygen reactor [8-9]. In this method, a portion of the oxygen gas generated by the oxygen reactor's decomposition process is heated to 530oC and reinjected into the oxygen reactor to transfer heat directly to the molten salt.

Research on bubble column reactors has been done both experimentally and numerically throughout the years. The Eulerian approach to CFD analyses for bubble column reactors has been reviewed by Abdulrahman et al. [10]. Abdulrahman [11–15] has examined the results of 2D CFD simulations for the bubble column reactor's gas holdup, volumetric heat transfer coefficient, gas and slurry temperatures, and solid concentration. Sarhan et al. [16] have investigated the effects of the physico-chemical properties of the liquid and gas phases on bubble formation and hydrodynamics of a bubble column reactor using the population balance equation combined with a 3D CFD model. They have used a Euler-Euler CFD model to predict experimental results of the gas holdup in a bubble column reactor using different phase flows within the range of ±7%. Also, they have observed that the gas holdup will increase slightly as the gas phase density increases. Li et al. [17] have conducted both experimental and CFD hydrodynamic analysis of an air- water- glass beads slurry bubble column. The slurry bubble column reactor was modeled using a 2D axisymmetric two fluid Euler k-Ɛ model. It was noted that the change of hydrodynamic characteristics with column diameters is the major cause of bubble column scale-up rules. Bubble columns with

wider reactor diameters result in the axial liquid velocity rising dramatically within the column core, while the gas holdup is very minimally influenced. Also, it was noted that with increasing column scales, turbulent kinetic energy rises.

Li and Zhong [18] conducted a 3D, Eulerian-Eulerian-Eulerian, three phase (air-water–glass powder), time dependent, CFD analysis of three different bubble column reactors to study the hydrodynamics in relation to time step, momentum discretization schemes and wall boundary conditions. The three different models used where the Gandhi et al. (height:2500mm, Static height: 1500mm diameter:150mm), the Rapure et al. model (height: 2000mm static height: 1000mm diameter:200mm) and the Li and Zhong model (height:800mm width: 100mm depth:10mm). The turbulence model used for their simulations was the RNG k-Ɛ model. Li and Zhong concluded that the conditions that best reflected experimental results were the use of a no slip condition, momentum discretization using the second order upwind, and a time step of 0.001s. Pu et al. [19] conducted a 2D CFD simulation of a molten salt bubble column, to investigate the hydrodynamics and direct heat transfer characteristics of a two-phase flow model (air – molten salt). An Euler- Euler multiphase model with a k-Ɛ turbulence model was used. Factors investigated during the simulation include changing the superficial gas velocity, varying the static liquid heights, and using different operational pressure and inlet gas temperature. It was observed that as the superficial gas velocity or the operational pressure increases so does the molten salt temperature and rising rate of the molten salt temperature over time. However, when the static liquid height rises, the rate of increase in average molten salt temperature falls. Increases in superficial gas velocity or operating pressure enhance the volumetric heat transfer coefficient, whereas increases in static liquid height lowers the volumetric heat transfer coefficient.

Zhang and Luo [20] generated a 2 phase (air-water) CFD model to investigate a bubble column's local gas-liquid slip velocity distribution in relation to heat transfer in a heterogeneous regime. The study also investigated the simulated time average of the local 2 phase slip velocities when varying superficial gas velocities, axial locations and scale of the bubble column. The model used was a CFD –PBM (population balance model) simulation with a RNG k-Ɛ turbulence. It was observed that raising the superficial gas velocities raised the local gas-liquid slip velocities in the region of developed flow. At larger superficial gas velocities, it was notices that the slip velocities were more affected by the radial position. The slip velocities near the center of the column where lower than that of the fully developed region. The slip velocities were minimally affected by the axial heights for the fully developed flow regions. Li et al [21] investigated the effects of a circular heat exchanger using a 2D CFD PBM model on the hydrodynamics of a pilot scale slurry bubble column reactor. A Euler –Euler multiphase model with an RNG k-Ɛ turbulence model was used. The reactor investigated had a diameter of 30cm, height of 200cm and the circular heat exchanger had a height of 108cm. Paraffin oil and catalyst particles where the assumed materials in the simulation. It was observed that the gas phase was notably distributed, local circular vertices were generated, and the slurry was strongly circulated due to the implementation of the circular heat exchanger tube. The bimodal profile of the gas holdup profile in the radial direction is caused by the circular gas distributor's particular layout. Furthermore, the circular heat exchanger tube increases this distribution, resulting in a larger gas holdup, which facilitates momentum transfer. Based on the above literature review, it can be concluded that the effect of static liquid height on gas holdup in the oxygen bubble column reactor of the Cu-Cl cycle for hydrogen production using 3D CFD simulations has not previously been investigated. This paper addresses the aforementioned gap.

2. CFD SIMULATION MODEL

The simulations of this thesis are validated against the experimental data provided by Abdulrahman [9, 22-25]. As such the simulated reactor is designed to be a simplified version of the physical reactor to reduce computational costs. The experimental reactor was constructed of stainless steel with a diameter of 21.6 cm. A stainless-steel distributor is inserted 10.8cm above the base of the SBCR. The gas was fed into the SBCR using a six-arm sparger type gas distributer. Each arm of the sparger had 12 orifices with 0.3cm diameters (72 holes in total). The orifices on the sparger were 4.4 cm, 5.5, 6, and 6.8cm from the center of the reactor [4] as seen in Fig. 1.

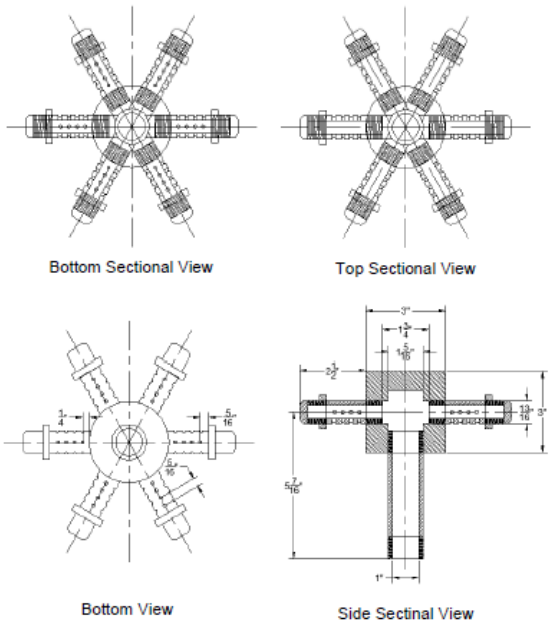

Fig. 1 Sparger design [9].

Initially the reactor and sparger designs were recreated using Inventor Professional. However, in order to reduce computational costs, the designs were simplified. First the sparger head was lowered by 10 cm so that the gas would be released at the base of the reactor. This would mean that the simulated heights (H) would be comparable to the experimental results that are 10cm higher. For example, the reactor heights in the simulations are 35, 45 and 55cm which were compared to the experimental results when the static liquid heights were 45, 55, and 65cm. The model could be further simplified to reduce computational costs. As such the sparger was simplified to a single inlet at the base of the reactor opposed to 72 inlets. The inlet has a diameter of 18cm and is extruded 0.3cm downward. The diameter for the gas inlet was selected to represent the bubble distribution at the base of the experimental reactor. The progression of the design simplification can be viewed in Fig. 2. The final reactor design can be seen in Fig. 3 with overall diameter 21.6 cm, gas inlet diameter18cm extruded 0.3cm downward with varying heights depending on the experiment.

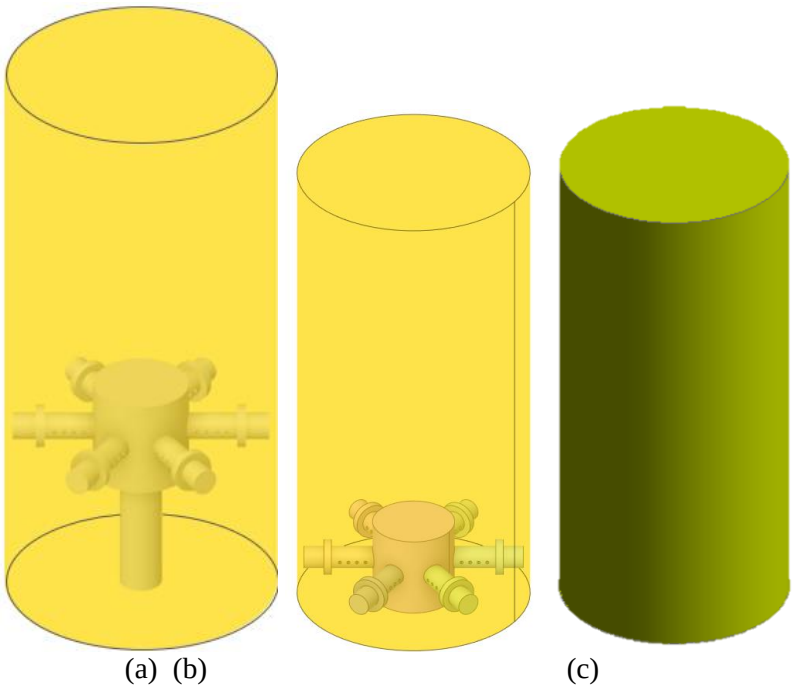

(a) (b) (c)

Fig. 2 Progression of simplifying the reactor design (a) most complex, (b) more simplified (c) most simple (final design).

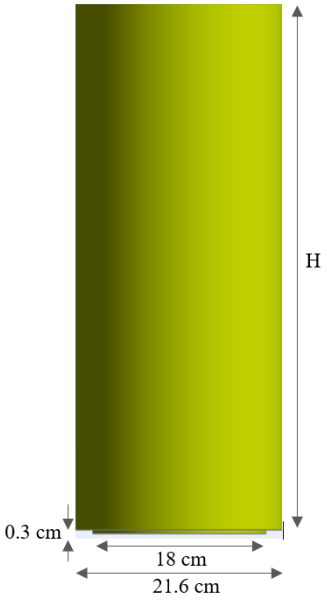

Fig. 3 Final SBCR geometry used for simulations.

Due to the difficulties associated with the Cuprous Chloride (CuCl) and Oxygen (O2) substances, Abdulrahman [9, 22-25] conducted his experiments on a Water-Helium-Alumina system. The challenges include the difficulty in observing O2 bubbles in molten CuCl because of its dark colour, the corrosiveness of the CuCl molten salt, and the O2 gas's ability to oxidize a variety of substances to accelerate its combustion [9, 26-27]. Based on the Buckingham pi theorem, a dimensional analysis revealed that liquid water at 22 oC and Helium gas at 90 oC are suitable substitutes for molten CuCl at 530 oC and oxygen gas at 600 oC [9]. In this paper, simulations of a 3D plane system are performed using an Eulerian-Eulerian model, an Eulerian sub-model, and a pressure-based solver type. The turbulence model used is RNG k-Ɛ model and the wall function is the standard wall function. For the BCR, a hexahedron mesh is used. The independence analyses of the mesh are performed to guarantee that the largest mesh size is chosen to minimize computational costs while achieving acceptable results. The mesh's final composition consists of 26,825 nodes and 24,396 elements. This resulted in a 3% difference in gas holdup when utilizing finer meshes. The inlet boundary condition is specified with an inlet superficial gas velocity and a gas holdup of 1. The pressure at the outlet is set to atmospheric pressure. For both phases, a no-slip condition is applied to the reactor's walls. It is challenging to estimate turbulent kinetic energy and dissipation rate at the inlet and outlet, so 5,000 iterations were used to specify them. Table 1 displays the equations used in the CFD analysis of this paper. The equations in Table 1 are written exclusively for the gas phase. Since the equations for liquid phase are similar to those for gas phase, they are not repeated.

Table 1: Details of equations used in the 3D CFD simulations.

Description [reference]	**Equation**
Volume equation [28]	$V_g = \int_V \alpha_g \, dV$
Continuity equation in 3D Polar coordinates (r, θ, y) [9]	$\nabla . V_g = \frac{\partial v_{r,g}}{\partial r} + \frac{v_{r,g}}{r} + \frac{1}{r}\frac{\partial v_{\theta,g}}{\partial \theta} + \frac{\partial v_{y,g}}{\partial y} = 0$

Momentum equation in 3D Polar coordinates [9]	$\rho_g \alpha_g (\frac{\partial v_r}{\partial t} + v_r \frac{\partial v_r}{\partial r} + \frac{v_\theta}{r}\frac{\partial v_r}{\partial \theta} + vy \frac{\partial v_r}{\partial y} - \frac{v_\theta^2}{r}) = -\alpha_g \frac{\partial P}{\partial r} + \alpha_g \frac{\mu_{g,eff}}{3}\frac{\partial(\nabla.V)}{\partial r} + \mu_{g,eff}\ \alpha_g [\frac{1}{r}\frac{\partial}{\partial r}(r\frac{\partial v_r}{\partial r}) + \frac{1}{r^2}\frac{\partial^2 v_r}{\partial \theta^2} + \frac{\partial^2 v_r}{\partial y^2} - \frac{v_r}{r^2} - \frac{2}{r^2}\frac{\partial v_\theta}{\partial \theta}] + \rho_g \alpha_g\ g_r + M_{i,g,r}$
	$\rho_g \alpha_g (\frac{\partial v_\theta}{\partial t} + v_r \frac{\partial v_\theta}{\partial r} + \frac{v_\theta}{r}\frac{\partial v_\theta}{\partial \theta} + v_y \frac{\partial v_\theta}{\partial y} + \frac{v_r v_\theta}{r}) = -\alpha_g \frac{1}{r}\frac{\partial P}{\partial \theta} + \alpha_g \frac{\mu_{g,eff}}{3r}\frac{\partial(\nabla.V)}{\partial \theta} + \alpha_g \mu_{g,eff} [\frac{1}{r}\frac{\partial}{\partial r}(r\frac{\partial v_\theta}{\partial r}) + \frac{1}{r^2}\frac{\partial^2 v_\theta}{\partial \theta^2} + \frac{\partial^2 v_\theta}{\partial y^2} + \frac{2}{r^2}\frac{\partial v_r}{\partial \theta} - \frac{v_\theta}{r^2}] + \rho_g \alpha_g\ g_\theta + M_{i,g,\theta}$
	$\rho_g \alpha_g (\frac{\partial v_y}{\partial t} + v_r \frac{\partial v_y}{\partial r} + \frac{v_\theta}{r}\frac{\partial v_y}{\partial \theta} + v_y \frac{\partial v_y}{\partial y}) = -\alpha_g \frac{\partial P}{\partial y} + \alpha_g\ \mu_{g,eff} [\frac{1}{r}\frac{\partial}{\partial r}(r\frac{\partial v_y}{\partial r}) + \frac{1}{r^2}\frac{\partial^2 v_y}{\partial \theta^2} + \frac{\partial^2 v_y}{\partial y^2}] + \rho_g \alpha_g g_y + M_{i,g,y}$
Energy equation in 3D Polar coordinates [9]	$\alpha_g \rho_g C\ (\frac{\partial T_g}{\partial t} + v_{r,g}\frac{\partial T_g}{\partial r} + \frac{v_{\theta,g}}{r}\frac{\partial T_g}{\partial \theta} + v_{y,g}\frac{\partial T_g}{\partial y}) = \bar{\bar{\tau}}_g : \nabla V_g + k_g (\frac{1}{r}\frac{\partial}{\partial r}(r\frac{\partial T_g}{\partial r}) + \frac{1}{r^2}\frac{\partial^2 Tg}{\partial \theta^2} + \frac{\partial^2 T_g}{\partial y^2}) + S_g + Q_{g,sl}$
Effective density	$\hat{\rho}_g = \alpha_g\ \rho_g$
Drag force [28]	$M_D = \frac{\rho_g f}{6\ \tau_b}\ d_b\ A_i\ (\boldsymbol{V_g} - \boldsymbol{V_l})$
Interfacial area [28]	$A_i = \frac{6\ \alpha_g\ (1-\alpha_g)}{d_b}$
Schiller-Naumann drag equation [29]	$C_D = \begin{cases} \frac{24\ (1+0.15\ Re_b^{0.687})}{Re_b} & Re_b \le 1000 \\ 0.44 & Re_b > 1000 \end{cases}$

3. Results

Figure 4 shows the three-dimensional gas holdup (α_g) versus static liquid height (H) and superficial gas velocity (U_{gs}) curves. The effects of varying H on α_g while changing the superficial gas velocity (U_{gs}) for a helium-water system are shown in Fig. 5. It can be observed from the graphs that increasing H decreases α_g. The contours of the cut section of the BCR taken in the center of the XY and ZY planes are shown in Figs. 6 and 7. Additional cut sections are taken at varying heights on the ZX plane within the reactor at heights of 10, 20, and 30 cm from the reactor's base in order to obtain a more precise profile of α_g. It is evident from the contours that the gas holdup is not symmetrical in the XY, ZY, and ZX planes, indicating that its behaviour is highly three-dimensional. It has been observed that as H increases, α_g decreases. At a superficial gas velocity of 0.05m/s, increasing H from 45cm to 65cm reduces the gas holdup by approximately 11%. With a superficial gas velocity of 0.15m/s, an increase in H from 45cm to 65cm resulted in a decrease of approximately 15% in the gas holdup. This is due to the increase in hydrostatic pressure and the decrease in pressure as H increases for specific U_{gs}. Additionally, having a shorter BCR (HR/DR < 3) can prevent the complete development of liquid circulation, thereby decreasing α_g [30].

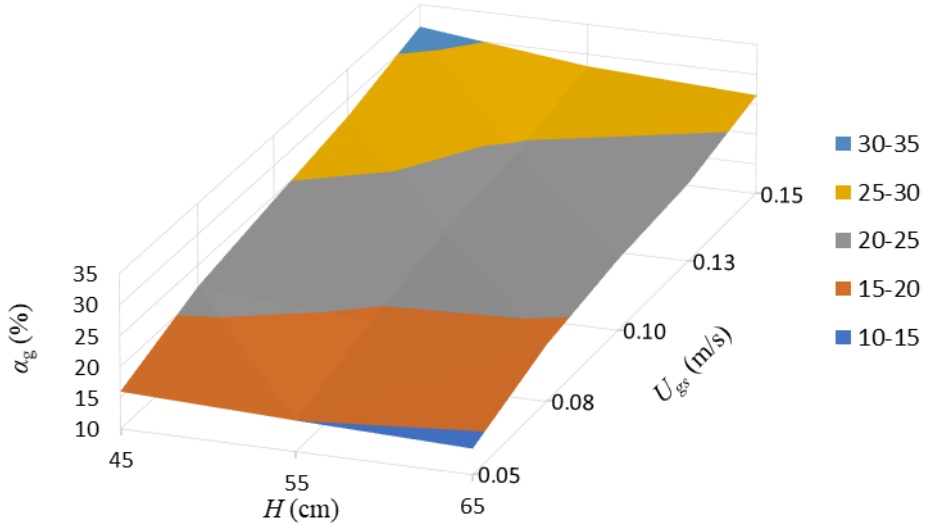

Fig. 4 Average Gas Holdup Versus Static Liquid Height and Superficial Gas Velocity of Helium-Water system.

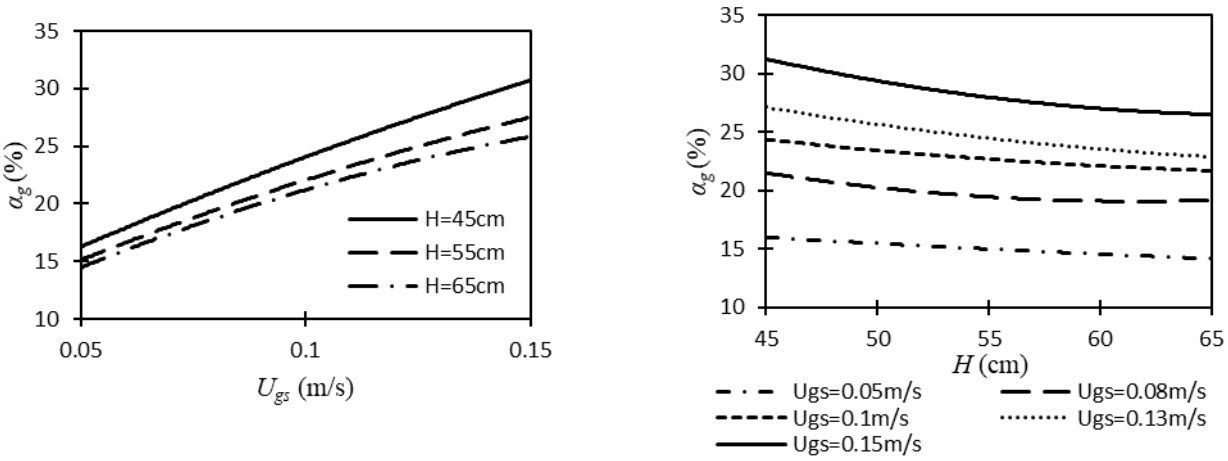

(a) (b)

Fig. 5 The effect of static liquid height on gas holdup for different superficial gas velocities.

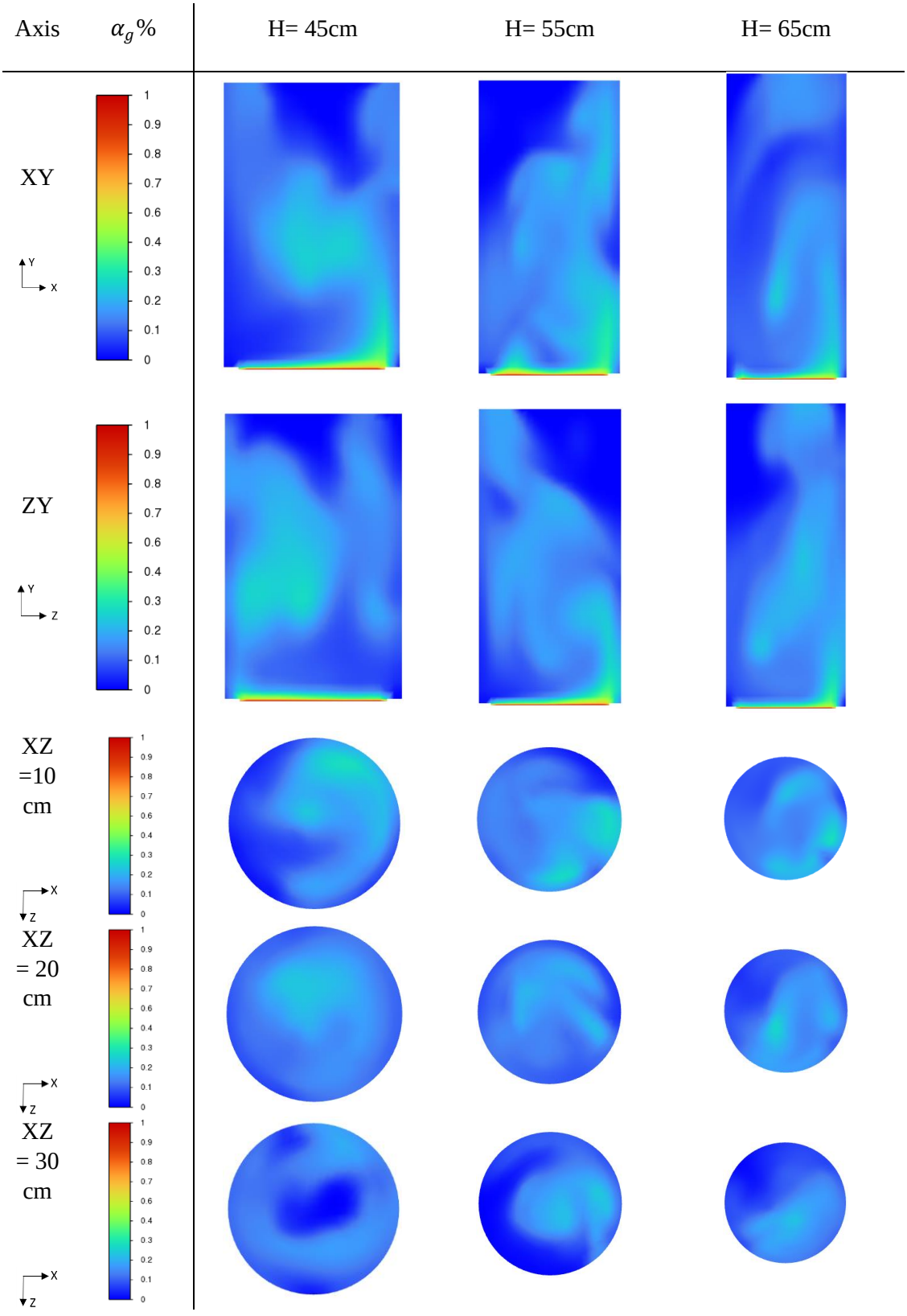

Fig. 6 Gas holdup contours for different static liquid heights and U_{gs} = 0.05 m/s.

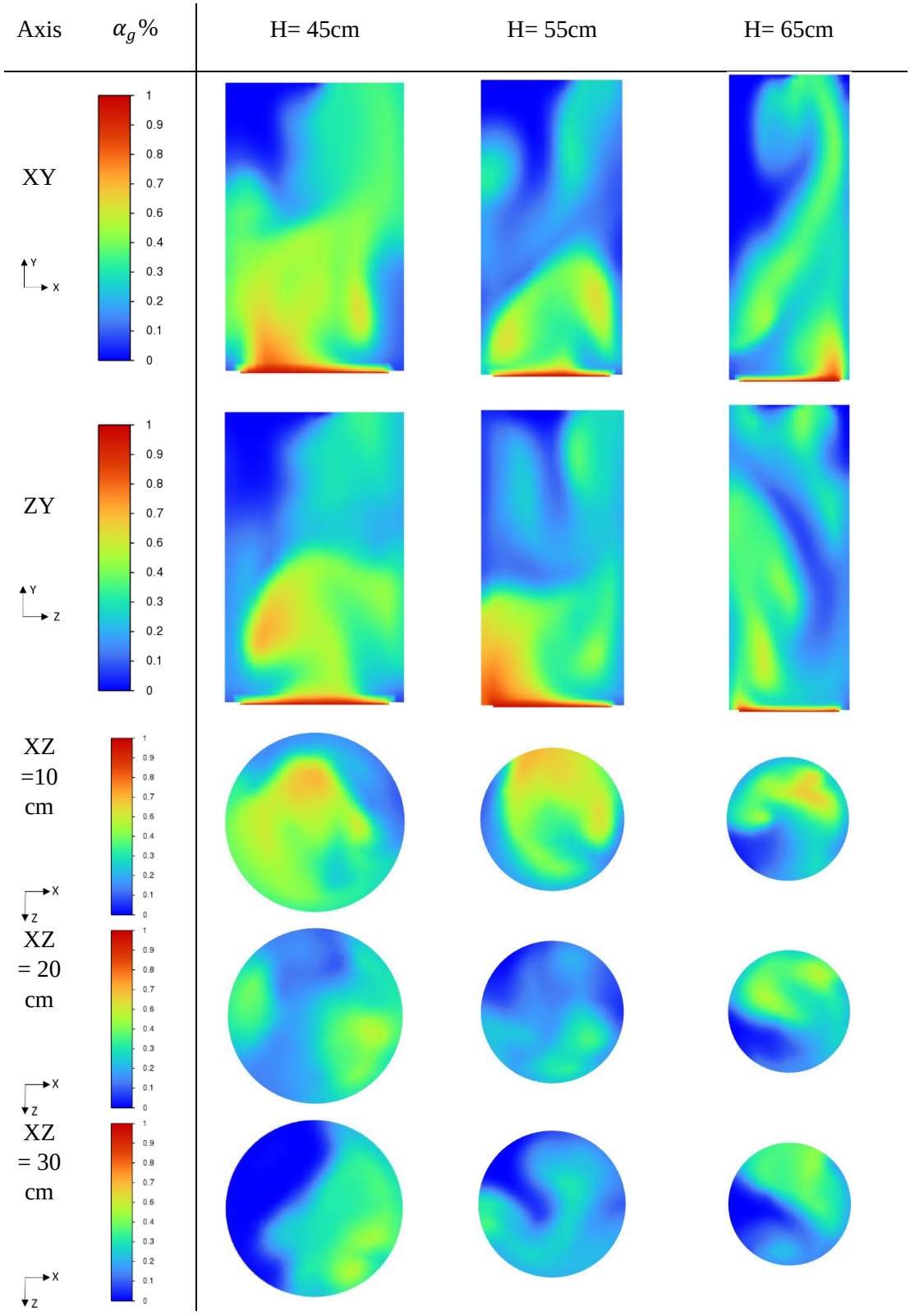

Fig. 7 Gas holdup contours for different static liquid heights and U_{gs} = 0.15 m/s.

The gas holdup results of the 3D-CFD Helium-Water BC simulations were validated against experimental data from Abdulrahman [9] (Fig. 8) and compared to 2D simulations from Abdulrahman [9] (Fig. 9). Figures 8 and 9 show the ability of the 3D-CFD models to determine the gas holdup (α_g) at various static liquid heights (H). Theoretical 3D-CFD models can predict the experimental data with reasonable accuracy. It can be observed that the majority of gas holdup simulation results were overestimated. Reducing the mesh size is one possible technique for minimizing relative error. The software will be able to account for minor vortical structures in the flow, such as eddies, if the mesh size is decreased [31].

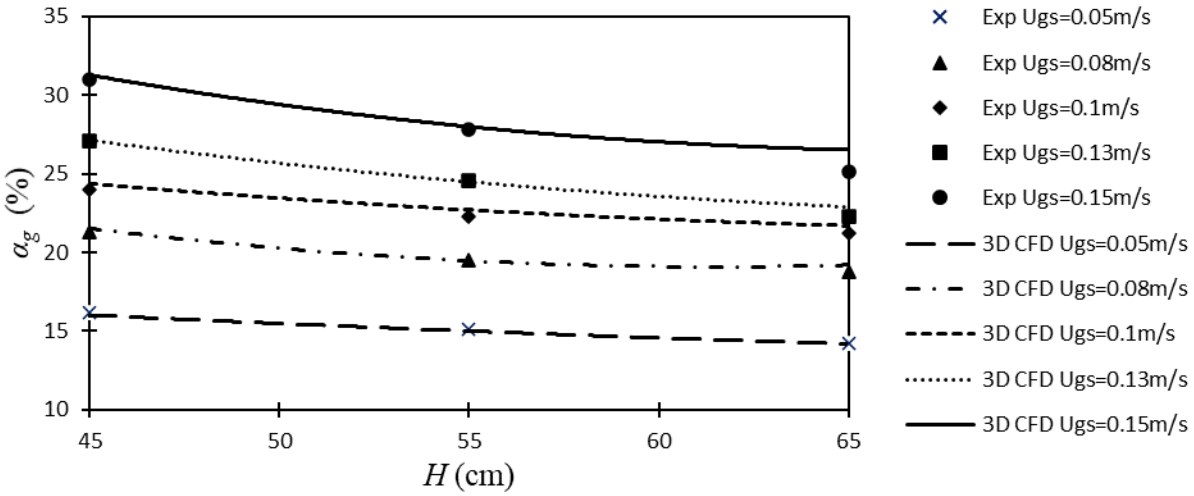

Fig. 8 Comparison of the average gas holdup versus static liquid height between 3D CFD simulations and experimental data.

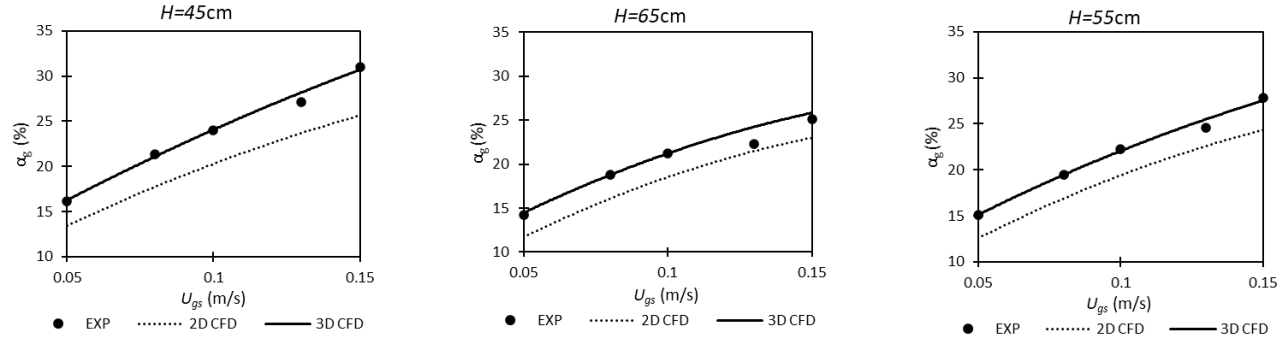

Fig. 9 Comparisons of the average gas holdup versus superficial gas velocity for different static liquid heights between 3D CFD simulations, 2D CFD simulations and experimental data.

5. Conclusions

This paper investigates 3D CFD analyses for the hydrodynamics of a bubble column reactor with direct contact heat transfer. The results of this paper demonstrates that gas holdup flow patterns in 3D CFD simulations are asymmetrical. Also, gas holdup increases as liquid height decreases. This is due to the increase in hydrostatic pressure and pressure drop that occurs when the static liquid height of the reactor increases at specific superficial gas velocity. With a superficial gas velocity of 0.05m/s, it is observed that increasing H from 45cm to 65cm decreases the gas holdup by 11%. Moreover, it is observed that the 3D-CFD results slightly overpredict the experimental results for gas holdup, whereas 2D simulations underpredict the experimental results. Finally, it is possible to conclude that 3D simulations are more accurate than 2D-CFD simulations.

List of Symbols

A_i	Interfacial area concentration	v	Velocity field

C		Specific heat		V_g	Volumes of gas
	C_D	Drag coefficient		V_l	Volumes of liquid
	d_b	Bubble diameter	U_{gs}		Superficial gas velocity
	g	Gravitational acceleration		α_g	Gas holdup
	H	Height	μ_{eff}		Effective viscosity
	Mi	Total interfacial forces between the phases	μ_g		Dynamic viscosity gas
	P	Phase pressure	μ_l		Dynamic viscosity liquid
$Q_{g,l}$		Intensity of heat exchange between the gas and liquid phases	ρ_g		Density, gas
	Re	Reynolds number	ρ_l		Density, liquid
	T	Temperature	$\bar{\bar{\tau}}:\nabla V$		Viscous stress tensor contracted with the velocity gradient

References

[1] Forsberg, Charles W. “Future Hydrogen Markets for Large-Scale Hydrogen Production Systems.” *International Journal of Hydrogen Energy*, vol. 32, no. 4, 2007, pp. 431–439.

[2] Lewis, Michele A., Manuela Serban, and John K. Basco. "Hydrogen production at 550 ºC using a low temperature thermochemical cycle." *Proc. Nuclear Production of Hydrogen: Second Information Exchange Meeting*. 2003.

[3] Serban, Manuela, Michele A. Lewis, and John K. Basco. *Kinetic study of the hydrogen and oxygen production reactions in the copper-chloride thermochemical cycle*. American Institute of Chemical Engineers, 2004.

[4] Abdulrahman, Mohammed W. "Similitude for Thermal Scale-up of a Multiphase Thermolysis Reactor in the Cu-Cl Cycle of a Hydrogen Production." *International Journal of Energy and Power Engineering*, vol. 10.5, 2016, pp. 664-670.

[5] Abdulrahman, Mohammed W. "Heat Transfer Analysis of a Multiphase Oxygen Reactor Heated by a Helical Tube in the Cu-Cl Cycle of a Hydrogen Production." *International Journal of Mechanical and Mechatronics Engineering*, vol. 10.6, 2016, pp. 1122-1127.

[6] Abdulrahman, M. W., Wang, Z., Naterer, G. F., & Agelin-Chaab, M. “Thermohydraulics of a thermolysis reactor and heat exchangers in the Cu-Cl cycle of nuclear hydrogen production.” in *Proceedings of the 5th World Hydrogen Technologies Convention,* 2013.

[7] Abdulrahman, Mohammed W. "Heat Transfer Analysis of the Spiral Baffled Jacketed Multiphase Oxygen Reactor in the Hydrogen Production Cu-Cl Cycle." In *Proceedings of the 9th International Conference on Fluid Flow, Heat and Mass Transfer (FFHMT’22)*, 2022.

[8] Abdulrahman, Mohammed W. "Review of the Thermal Hydraulics of Multi-Phase Oxygen Production Reactor in the Cu-Cl Cycle of Hydrogen Production." In *Proceedings of the 9th International Conference on Fluid Flow, Heat and Mass Transfer (FFHMT’22)*, 2022.

[9] Abdulrahman, Mohammed W. *Analysis of the thermal hydraulics of a multiphase oxygenproduction reactor in the Cu-Cl cycle*. Diss. University of Ontario Institute of Technology (Canada), 2016.

[10] Abdulrahman, Mohammed W., and Nibras Nassar. "Eulerian Approach to CFD Analysis of a Bubble Column Reactor–A." In *Proceedings of the 8th World Congress on Mechanical, Chemical, and Material Engineering (MCM'22)*, 2022.

[11] Abdulrahman, Mohammed W. “CFD Simulations of Gas Holdup in a Bubble Column at High Gas Temperature of a Helium-Water System.” In *Proceedings of the 7th World Congress on Mechanical, Chemical, and Material Engineering (MCM'20),* 2020

[12] Abdulrahman, M.W. “CFD Simulations of Direct Contact Volumetric Heat Transfer Coefficient in a Slurry Bubble Column at a High Gas Temperature of a Helium–Water–Alumina System.” *Applied Thermal Engineering*, vol. 99, 2016, pp. 224–234.

[13] Abdulrahman, Mohammed W. "CFD Analysis of Temperature Distributions in a Slurry Bubble Column with Direct Contact Heat Transfer." In *Proceedings of the 3rd International Conference on Fluid Flow, Heat and Mass Transfer (FFHMT’16)*. 2016.

[14] Abdulrahman, Mohammed W. “Temperature profiles of a direct contact heat transfer in a slurry bubble column.” *Chemical Engineering Research and Design,* vol. 182, 2022, pp. 183-193.

[15] Abdulrahman, Mohammed W. “Effect of Solid Particles on Gas Holdup in a Slurry Bubble Column.” In *Proceedings of the 6th World Congress on Mechanical, Chemical, and Material Engineering*, 2020.

[16] Sarhan, A.R., et al. “CFD Modeling of Bubble Column: Influence of Physico-Chemical Properties of the Gas/Liquid Phases Properties on Bubble Formation.” *Separation and Purification Technology*, vol. 201, 2018, pp. 130–138.

[17] Li, Zhaoqi, et al. “Experimental and Numerical Investigations of Scale-up Effects on the Hydrodynamics of Slurry Bubble Columns.” *Chinese Journal of Chemical Engineering*, vol. 24, no. 8, 2016, pp. 963–971.

[18] Li, Weiling, and Wenqi Zhong. “CFD Simulation of Hydrodynamics of Gas–Liquid–Solid Three-Phase Bubble Column.” *Powder Technology*, vol. 286, 2015, pp. 766–788.

[19] Pu, Wenhao, et al. “Simulation on Direct Contact Heat Transfer in Gas-Molten Salt Bubble Column for High Temperature Solar Thermal Storage.” *International Communications in Heat and Mass Transfer*, vol. 104, 2019, pp. 51–59.

[20] Zhang, Xi-Bao, and Zheng-Hong Luo. “Local Gas–Liquid Slip Velocity Distribution in Bubble Columns and Its Relationship with Heat Transfer.” *AIChE Journal*, vol. 67, no. 1, 2020.

[21] Li, Le, et al. “CFD-PBM Investigation of the Hydrodynamics in a Slurry Bubble Column Reactor with a Circular Gas Distributor and Heat Exchanger Tube.” *Chemical Engineering Science: X*, vol. 9, 2021, p. 100087.

[22] Abdulrahman, M. W. "Experimental studies of gas holdup in a slurry bubble column at high gas temperature of a helium− water− alumina system." *Chemical Engineering Research and Design* vol. 109, 2016, pp. 486-494.

[23] Abdulrahman, M. W. "Experimental studies of the transition velocity in a slurry bubble column at high gas temperature of a helium–water–alumina system." *Experimental Thermal and Fluid Science*, vol. 74, 2016, pp. 404-410.

[24] Abdulrahman, M. W. "Experimental studies of direct contact heat transfer in a slurry bubble column at high gas temperature of a helium–water–alumina system." *Applied Thermal Engineering*, vol. 91, 2015, pp. 515-524.

[25] Abdulrahman, Mohammed Wassef. "Direct contact heat transfer in the thermolysis reactor of hydrogen production Cu—Cl cycle." U.S. Patent No. 10,059,586. 28 Aug. 2018.

[26] Abdulrahman, Mohammed Wassef. "Material substitution of cuprous chloride molten salt and oxygen gas in the thermolysis reactor of hydrogen production Cu—Cl cycle." U.S. Patent No. 10,526,201. 7 Jan. 2020.

[27] Abdulrahman, Mohammed W. "Simulation of Materials Used in the Multiphase Oxygen Reactor of Hydrogen Production Cu-Cl Cycle." *Proceedings of the 6 the International Conference of Fluid Flow, Heat and Mass Transfer (FFHMT'19)*. 2019.

[28] *ANSYS FLUENT Theory Guide*, Release 14.5. (2012). ANSYS, Inc.

[29] L. Schiller, A. Naumann, Uber die grundlegenden berechnungen bei der schwerkraftaufbereitung / About the basic calculations in the gravity-treatment, Zeitung des vereins deutscher ingenieure / Newspaper of the Association of German Engineers, 1933, pp. 77–318.

[30] Behkish, Arsam. *Hydrodynamic and mass transfer parameters in large-scale slurry bubble column reactors*. Diss. University of Pittsburgh, 2005.

[31] Sokolichin, A., and Gs Eigenberger. "Applicability of the standard k–ε turbulence model to the dynamic simulation of bubble columns: Part I. Detailed numerical simulations." *Chemical Engineering Science* 54.13-14 (1999): 2273-2284.